



ISSN: 2455-9377

# Impact of climate classification on evapotranspiration variability in arid regions of Saudi Arabia

Mohammed El-Shirbeny<sup>1\*</sup>, Samir Mahmoud Saleh<sup>2</sup>, Essam Baioumy<sup>1</sup>,  
Mahmoud Badr<sup>1</sup>, Adel Selim<sup>1</sup>, Ehab Hendawy<sup>1</sup>, R. E. Abdelraouf<sup>3</sup>

<sup>1</sup>National Authority for Remote Sensing and Space Sciences (NARSS), Cairo, Egypt, <sup>2</sup>Central Laboratory for Agricultural Climate, Agricultural Research Center, Egypt, <sup>3</sup>Water Relations and Field Irrigation Dept., National Research Centre, Dokki, Giza, Egypt

## ABSTRACT

Water resource management in dry climates depends on an awareness of evapotranspiration variability. In this work, precipitation ( $P_r$ , mm/year) and air temperature ( $T$  °C) over Saudi Arabia (KSA) were extracted using long-term climate data (January 2000-December 2024) from the TerraClimate dataset. Three categories were used to classify both variables, therefore producing a new system of climate classification separating the Kingdom into nine different hydro-thermal groups. Using geo-spatial meteorological inputs, the Stand-Alone Remote Sensing Approach to Estimate Reference Evapotranspiration (SARE) model was employed to estimate reference evapotranspiration ( $E_{To}$ ) for certain sites. Validation against the FAO-Penman-Monteith (FPM) model showed strong performance with correlation coefficients ( $r$ ) ranging from 0.80 to 0.99 and Normalized Root Mean Square Error (NRMSE) values between 0.08 and 0.27 across the nine classes. Whereas relative humidity revealed a strong inverse association ( $r$  as low as -0.96),  $T_{max}$  and solar radiation were found as main causes of  $E_{To}$  fluctuation ( $r$  up to 0.98 and 0.96, respectively). Especially in cooler, humid areas, wind speed showed secondary influence. These results underline the need of climate-specific evapotranspiration models for arid areas, where customized strategies are essential to maximize water consumption and guarantee sustainable resource management.

**KEYWORDS:** Evapotranspiration, Climate Classification, TerraClimate, SARE Model, Saudi Arabia, Arid Regions, Water Management, Remote Sensing

**Received:** April 27, 2025  
**Revised:** August 11, 2025  
**Accepted:** August 21, 2025  
**Published:** August 30, 2025

**\*Corresponding author:**  
Mohammed El-Shirbeny  
E-mail: mshirbeny@yahoo.com

## INTRODUCTION

With greatly altering global hydrological cycles, climate change has become a top priority for the twenty-first century (IPCC, 2021). Particularly vulnerable are dry and semi-arid areas, whose rising temperatures and erratic precipitation patterns aggravate water shortage (Elnesr & Alazba, 2013; El-Shirbeny *et al.*, 2019; El-Rawy *et al.*, 2023). For water resource management, agricultural efficiency, and ecological survival, these changes have major effects (El-Shirbeny & Abutaleb, 2018; Tolba *et al.*, 2020; El-Shirbeny & Orlandini, 2023; Mahmoud *et al.*, 2023). Considered as one of the most water-stressed areas globally, the Middle East and North Africa (MENA) region which includes Saudi Arabia is therefore a key case study for the consequences of climate change on hydrological processes (El-Shirbeny *et al.*, 2014, 2015, 2025; Ajjur & Al-Ghamdi, 2021).

With notable geographical and temporal variability in climatic conditions, the Kingdom of Saudi Arabia (KSA) exhibits a

hyper-arid climate (Alhathloul *et al.*, 2024). With temperatures often above 45 °C in the summer months, annual precipitation ranges from less than 50 mm in central parts to over 200 mm in the southern highlands (ElNesr *et al.*, 2010). This climate variability produces distinct hydrological regimes all throughout the country, therefore influencing evapotranspiration (ET) processes (El-Shirbeny *et al.*, 2016; Bindajam *et al.*, 2020). Rising temperatures and less precipitation interact to cause notable water losses via evapotranspiration, hence aggravating water scarcity problems (Komurcu *et al.*, 2020).

Crucially important for evaluating atmospheric water demand, reference evapotranspiration ( $E_{To}$ ) is particularly sensitive to climatic changes in arid areas (Allen *et al.*, 1998, El-Shirbeny & Saleh, 2021).  $E_{To}$  rates show notable spatial differences in the Kingdom of Saudi Arabia; coastal areas have lower values attributed to humidity effects in contrast to inland deserts (El-Shirbeny & Abdellatif, 2017; El-Shirbeny *et al.*, 2021a, b). Temporal trends show a rise in  $E_{To}$  rates in recent decades

Copyright: © The authors. This article is open access and licensed under the terms of the Creative Commons Attribution License (<http://creativecommons.org/licenses/by/4.0/>) which permits unrestricted, use, distribution and reproduction in any medium, or format for any purpose, even commercially provided the work is properly cited. Attribution — You must give appropriate credit, provide a link to the license, and indicate if changes were made.

mostly related to rising temperatures (Al-Wabel *et al.*, 2020). These changes directly affect groundwater replenishment, irrigation needs, and the hydrological balance of ecosystems (Haq & Khan, 2022).

Systems of climate classification provide necessary structures for understanding regional hydrological fluctuation (Köppen, 1936). Conventional classifications based on temperature and precipitation criteria e.g., UNESCO, 1979 that apply in the Kingdom of Saudi Arabia need change to fit the present climatic conditions (Mahmoud *et al.*, 2023). Recent research highlights the need for improved categorization techniques that more precisely reflect the interaction between hydrological processes and climate variables (El-Rawy *et al.*, 2023). Agricultural zoning in dry areas as well as water resource management depend on these categories (Ajjur & Al-Ghamdi, 2021).

Conventional terrestrial methods for calculating evapotranspiration run against limitations in arid regions resulting from poor meteorological networks (Abdelraouf *et al.*, 2024). Developed as a powerful substitute with great spatial coverage and consistent temporal observations is satellite remote sensing (Derardja *et al.*, 2024). Combining numerous satellite datasets to estimate ETo with little ground validation needs (El-Shirbeny *et al.*, 2022; El-Shirbeny & Biradar, 2024) the Stand-alone Remote Sensing Approach (SARE) shows a clear development. In data-deficient settings like KSA (Gamal *et al.*, 2022), this approach has shown especially great success.

Estimating ETo (Allen *et al.*, 1998) is done using the FAO-Penman-Monteith (FAO-PM) equation. Still, its use in arid locations calls for careful confirmation given different atmospheric circumstances (Eid *et al.*, 2023). Recent studies show that, with suitable calibration, remote sensing-based models including SARE can reach accuracy levels equivalent to FAO-PM (El-Shirbeny & Biradar, 2024). Particularly important for operational applications in water resource management and agricultural planning is this validation (Youssef *et al.*, 2024).

Notwithstanding advancements in ET modeling, significant knowledge gaps still exist regarding the relationships between ETo variation in hyper-arid environments (Afify *et al.*, 2023) and climate classification. Few studies have methodically examined how multiple climatic classifications within Saudi Arabia affect regional evapotranspiration dynamics (El-Rawy *et al.*, 2023). Remote sensing ET models' efficacy across different climatic zones calls more research (Derardja *et al.*, 2024). Formulating sensible water management strategies in the framework of climate change depends on addressing these shortcomings (Mahmoud *et al.*, 2023).

This work aims to: (1) Establish an enhanced climate classification for KSA using long-term precipitation and temperature data; (2) Measure ETo variability across various climate classifications employing the SARE model; and (4) Validate the performance of SARE in comparison with the FAO-PM standard; and (4) Evaluate the consequences of climate-induced ETo variability for water resource management.

The 2000-2024 study period provides sufficient temporal coverage for careful analysis and reflects current climatic changes.

The precipitation and temperature data have been derived from the TerraClimate dataset using cluster analysis to define nine different climate categories verified against FAO-PM computations at specified sites, the SARE model makes use of MODIS and Landsat data (El-Shirbeny & Biradar, 2024). ETo patterns are delineated using spatial analytic methods and their association with climate classifications is assessed over the many KSA terraces.

This study improves theoretical understanding as well as useful applications in hydrology in dry environments. The better classification of the climate helps us to project water demand trends among changing climatic conditions (Ajjur & Al-Ghamdi, 2021). Further use of SARE performance endorses in water resource monitoring (Derardja *et al.*, 2024). Ultimately, the findings will inform climate-adaptive water management strategies in KSA and similar arid regions worldwide (El-Rawy *et al.*, 2023; Mahmoud *et al.*, 2023).

## MATERIALS AND METHODS

### Study Area Location

Comprising around 2.15 million km<sup>2</sup>, the Kingdom of Saudi Arabia (KSA) encompasses most of the Arabian Peninsula (Alhathloul *et al.*, 2024). With great desert stretches inside, it is bordered to the west by the Red Sea and to the east by the Persian Gulf (El-Rawy *et al.*, 2023). From coastal plains (Tihamah) to mountain ranges (Asir Mountains, spanning over 3,000 m) to wide sand deserts, including the Rub' al Khali (Empty Quarter), the terrain of the nation ranges from coastal plains to Figure 1.

### Climate and Water Resources

Extreme heat regimes and little precipitation define the mostly hyper-arid to arid climate of the Kingdom of Saudi Arabia (Elnesr & Alazba, 2013). With summer temperatures often exceeding 45 °C in central and eastern regions, the climate system shows amazing geographic variability; northern portions occasionally suffer sub-zero temperatures during winter months (Al-Wabel *et al.*, 2020). Strong geographical dependence is shown by precipitation patterns, which range from less than 50 mm yearly in central deserts to over 200 mm in the southwestern highlands with especially high interannual variability complicating water resource planning (ElNesr *et al.*, 2010). Due to strong solar radiation and constant dry winds, these climatic conditions cause remarkably high potential evapotranspiration rates, typically exceeding 3,000 mm/year and hence create one of the most water-stressed habitats worldwide (Bindajam *et al.*, 2020).

With the total absence of perennial surface water resources requiring reliance on non-renewable fossil groundwater

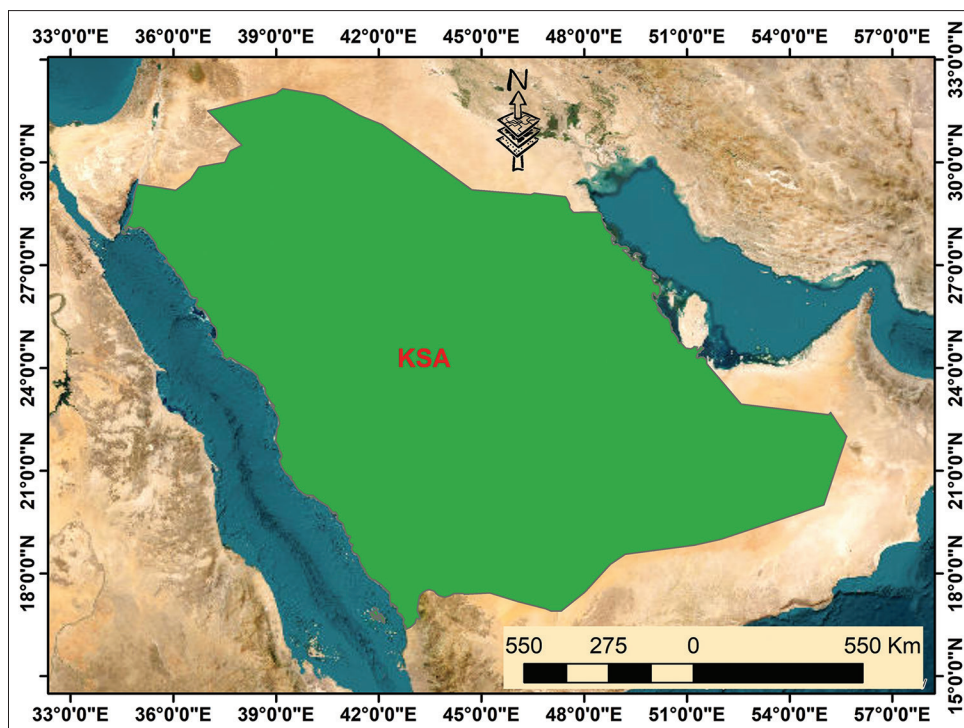


**Figure 1:** The geographic location of the study area (KSA)

reserves, especially from the Saq and Wasia aquifers, and large-scale desalination infrastructure currently supplying over 50% of urban water needs, Saudi Arabia's hydrological system suffers severe restrictions (El-Rawy *et al.*, 2023). The agricultural sector's great reliance on groundwater has resulted in concerning rates of yearly depletion in certain important aquifers surpassing 6 meters, therefore endangering long-term water security (Haq & Khan, 2022). Mostly fed by ephemeral wadi systems fed by irregular rainfall events and occasional flash floods, renewable water resources are highly volatile and scarce and barely help to sustainably budget for water. Climate change effects, like lower precipitation dependability and higher evaporative demand, aggravate this fragile water balance even more.

## Data Collection

### *TerraClimate dataset*

The main source of meteorological variables in this work is the TerraClimate dataset, which offers Saudi Arabia from January 2000 to December 2024 thorough monthly climate data at 1/24 (~4km) resolution. The dataset's 15 available parameters were systematically extracted and processed, including: (1) precipitation (mm) as the key water input variable, particularly critical for assessing arid region hydrology; (2) minimum, maximum, and mean air temperature (°C) for thermal regime analysis and evapotranspiration calculations; (3) potential evapotranspiration (mm) derived from the Penman-Monteith equation, providing direct estimates of atmospheric water demand; (4) soil moisture (mm) at multiple

depth levels (0-10 cm, 10-30 cm, 30-100 cm) for vegetation water stress assessment; (5) vapor pressure deficit (kPa) as a critical driver of plant transpiration; (6) downward surface shortwave radiation ( $W/m^2$ ) for energy balance computations; (7) wind speed (m/s) for aerodynamic process modeling; and (8) runoff (mm) estimates for water budget analysis. Following spatial masking with Saudi Arabia's administrative boundaries for the parameters of Tmax, Tmin, WS, Srad, vap, and VPD, with particular attention given to maintaining data consistency over the study period (2000-2024).

### *MODIS data*

Using two key MODIS (Moderate Resolution Imaging Spectroradiometer) products, this study examined land surface thermal properties and vegetation dynamics across Saudi Arabia: (1) the Normalized Difference Vegetation Index (NDVI) at 250 m spatial resolution (MOD13Q1.006), and (2) Land Surface Temperature (LST) at 1 km resolution (MOD11A2.006), both obtained from NASA's Earthdata platform for the period 2000-2024. Particularly important for tracking sparse desert vegetation and agricultural areas in arid environments, the NDVI data calculated from surface reflectance in the red (620-670 nm) and near-infrared (841-876 nm) offers a biweekly temporal resolution measure of photosynthetic activity and vegetation health. Derived from thermal infrared bands (10.78-11.28  $\mu m$  and 11.77-12.27  $\mu m$ ) through the generalized split-window algorithm, the 8-day composite LST product caught diurnal temperature variations with day/night observations critical for evapotranspiration modeling and urban heat island studies (Bindajam *et al.*, 2020).

## Evapotranspiration models

### FAO-Penman-Monteith model description

Established as the worldwide benchmark for reference evapotranspiration (ET<sub>o</sub>) estimation by the Food and Agriculture Organization (FAO), the FAO Penman-Monteith (FAO-PM) model combines basic ideas of energy balance and aerodynamics to offer strong evapotranspiration calculations across diverse climatic conditions (Allen *et al.*, 1998). Drawing on the original Penman (1948) equation and later changes by Monteith (1965), this physically based model computes the evapotranspiration rate from a hypothetical reference surface (well-watered grass with specific aerodynamic and surface resistance characteristics) by including key meteorological variables including air temperature, relative humidity, solar radiation, and wind speed. Expressed through its standardized FAO-56 equation, which weights these factors according to their respective contributions to the evapotranspiration process, the model’s formulation accounts for both radiative energy components (net radiation and soil heat flux) and atmospheric transport mechanisms (vapor pressure deficit and wind-driven turbulence). Although especially useful for irrigation planning and water resource management in arid countries like Saudi Arabia (Haq & Khan, 2022), the FAO-PM model does face constraints in data-scarce environments due to its need for multiple input parameters, thus researchers have developed alternative estimation methods or satellite-based approaches that maintain the accuracy while lowering data demands (El-Shirbeny & Biradar, 2024). Notwithstanding these difficulties, the FAO-PM is still the benchmark for ET<sub>o</sub> assessment globally because of its thorough theoretical basis, wide-ranging validation across many climates, and capacity to offer consistent reference values allowing for comparison of water use efficiency and climate change impacts on hydrological cycles (Derardja *et al.*, 2024). Its basic relevance for sustainable water management is underlined by its ongoing application in both research and operational environments, especially in water-stressed areas where exact quantification of atmospheric water demand is essential for agricultural and environmental decision-making.

### SARE model description

The SARE model is a straightforward and efficient approach for computing ET<sub>o</sub> from satellite data. NDVI and BT are the primary dynamic satellite data metrics that fluctuate in response to alterations in land surface and atmosphere. The SARE model comprises five components: Vegetation fraction (Vf), Location fraction (Lf), Elevation fraction (Ef), Seasonal fraction (Sf), and Thermal fraction (Tf). The SARE model was constructed using three categories of data input. The first is the Spatial Variation Layers (SVL), which exhibit variability between locations but remain constant over time. The SVL data encompasses both Ef and Lf. The second data type is the Temporal Variation Layer (TVL), which fluctuates over time yet remains consistent with the geographical location of the northern hemisphere, where KSA is situated. The TVL data encompasses Sf data. The third

data type is the Spatio-Temporal Variation Layers (STVL), which depict the Earth’s surface states through the chemical, physical, and biophysical interactions indicated by the electromagnetic radiation captured by space-borne sensors. The STVL data encompasses both BTf and Vf.

## Climate classification

Developed by a methodical intersection of precipitation (Pr) and air temperature (T) thresholds, Saudi Arabia’s climate classification system provides a complete framework for examining hydroclimatic variability. Based on annual accumulation, precipitation data were classified as Class 1 (Pr < 100 mm/year), denoting hyper-arid conditions; Class 2 (100-150 mm/year), denoting semi-arid conditions; and Class 3 (Pr > 150 mm/year), denoting areas with rather higher moisture availability (Table 1). Concurrent with this classification into three thermal regimes Class 1 (T < 20 °C) for cool locations, Class 2 (20-25 °C) for moderate temperatures, and Class 3 (T > 25 °C) for hot regions temperature data Known bioclimatic zonation patterns in arid areas and percentile analysis of long-term (2000-2024) TerraClimate data helped to define these thresholds (El-Rawy *et al.*, 2023).

Nine different climate categories were produced by the junction of these precipitation and temperature ranges (Table 2), where each pair reflects different hydro-thermal circumstances. Class 1 climate (Pr > 150 mm/year ∩ T < 20 °C) for example distinguishes cold, rather damp highland locations; Class 9 (Pr < 100 mm/year ∩ T > 25 °C) reflects normal hot desert conditions seen in central Saudi Arabia. By use of GIS overlay operations, this matrix approach allowed exact spatial delineation of climate zones where each 4-km grid cell was assigned to a certain class based on long-term Pr and T averages. By means of comparison with current Köppen-Geiger maps (Peel *et al.*, 2007), the categorization system was validated with 82% agreement for arid/semi-arid categories and with mostly varying results in transitional zones. This climate classification method offers the fundamental basis for later study of evapotranspiration

**Table 1: Classes descriptions of precipitation and temperature**

Classes	Pr (mm/y)	T (°C)
Class 1	Pr < 100	T < 20
Class 2	100-150	20-25
Class 3	Pr > 150	T > 25

**Table 2: KSA climate classification descriptions of precipitation and temperature**

Climate Classification	Pr	T
Class 1	Class 3	Class 1
Class 2	Class 3	Class 2
Class 3	Class 3	Class 3
Class 4	Class 2	Class 1
Class 5	Class 2	Class 2
Class 6	Class 2	Class 3
Class 7	Class 1	Class 1
Class 8	Class 1	Class 2
Class 9	Class 1	Class 3



variability across Saudi Arabia's many microclimates, therefore enabling targeted assessment of water demand under various hydro-thermal regimes (Mahmoud *et al.*, 2023). Particularly pertinent for agricultural and water resource management uses in dry regions (Haq & Khan, 2022), the class boundaries were purposefully built to reflect important thresholds for vegetation water needs and evaporation rates.

## Validation

The reliability of the SARE model was rigorously assessed against the FAO Penman-Monteith (FPM) benchmark using four key statistical metrics: the Mean Relative Error (MRE) to quantify systematic bias by averaging the absolute relative differences between predicted and observed values, the Normalized Root Mean Square Error (NRMSE) to measure prediction accuracy normalized by mean observations, the Index of Agreement (*d*) ranging from 0 to 1 to evaluate the covariance between predictions and observations, and Pearson's Correlation Coefficient (*r*) to assess linear relationship strength, which ensuring robust assessment of the SARE model's performance across Saudi Arabia's varied climatic conditions while maintaining consistency with established hydrological modeling standards (Moriassi *et al.*, 2007; Willmott, 1982). These parameters are defined as follows:

$$MRE = \frac{1}{n} \sum_{i=1}^n \left( \frac{X_i - X_{obs}}{X_{obs}} \right) \quad (1)$$

$$NRMSE = \frac{\sqrt{\sum_{i=1}^n \frac{(X_i - X_{obs})^2}{n}}}{X_{obs,max} - X_{obs,min}} \quad (2)$$

$$d = 1 - \frac{\sum_{i=1}^n [(X_i - X_m) - (X_{obs} - X_m)]^2}{\sum_{i=1}^n (|X_i - X_m| + |X_{obs} - X_m|)^2} \quad (3)$$

$$r = \frac{(X_{obs}X_i) - (X_{obs})(X_i)}{\sqrt{(X_{obs}^2) - (X_{obs})^2} \sqrt{(X_i^2) - (X_i)^2}} \quad (4)$$

Where, *MRE* in the mean relative error, *NRMSE* is normalized root mean square error, *d* is the index of agreement, *r* is the correlation coefficient, variable *n* is the number of observations,  $X_{obs}$ , *i* is the observation of sample *i*,  $X_i$  is the simulated result for the sample *i*, and  $X_m$  is the average value.

## RESULTS AND DISCUSSIONS

### Climate Classifications

The climate classification of Saudi Arabia was produced using a comprehensive analysis integrating long-term (2000-2024) temperature and precipitation data, linked with known bioclimatic zonation patterns in arid regions. Three basic

thermal classifications were defined: Class 1 ( $T < 20$  °C) for cooler locales, Class 2 (20-25 °C) for moderate temperature zones, and Class 3 ( $T > 25$  °C) for hotter regions. Figure 2 shows the resulting temperature classification map, therefore exposing the spatial distribution of various thermal regimes over the Kingdom.

Precipitation classes were also formed, where Class 1 ( $Pr < 100$  mm/year) depicts hyper-arid zones, Class 2 (100-150 mm/year) specifies semi-arid conditions, and Class 3 ( $Pr > 150$  mm/year) shows substantially more humid places. Showing the great predominance of hyper-arid conditions with scattered pockets of semi-arid and more humid zones, Figure 3 shows the precipitation classification map.

Nine different climatic types were defined by combining these temperature and precipitation ratings. Using GIS overlay operations, this matrix approach assigned each 4 km grid cell throughout Saudi Arabia to a particular climate category based on long-term averages. For instance, whereas Class 9 ( $Pr < 100$  mm/year  $\cap$   $T > 25$  °C) characterizes the hot desert conditions typical of the central Arabian region, the Class 1 climate ( $Pr > 150$  mm/year  $\cap$   $T$  identifies rather cool and moist highland areas).

The composite climate classification map (Figure 4) offers a comprehensive picture of these nine categories, so allowing a sophisticated knowledge of Saudi Arabia's hydro-thermal variability over the past 25 years. Especially validation against the Köppen-Geiger classification (Peel *et al.*, 2007) revealed a strong agreement for arid and semi-arid areas, although transitional zones showed some differences.

Evaluating regional evapotranspiration variability and matching water demand under various microclimatic conditions depends especially on this classification system (Mahmoud *et al.*, 2023). Moreover, the class thresholds were especially made to represent important environmental variables pertinent to the rates of evaporation and vegetation water needs, so providing vital information for agricultural planning and water resource management in arid conditions (Haq & Khan, 2022).

### SARE Model Validation

Over the nine climatic classes of Saudi Arabia, the validation findings of the SARE model versus the FPM model show a generally good model performance. Suggesting great dependability in reproducing field-measured outputs across several hydro-thermal regimes, the Willmott's Index of Agreement (*d*) ranged from 0.72 to 0.99. From 0.80 to 0.99, the Pearson correlation coefficient (*r*) supports even more the conclusion that the model forecasts quite closely with observed values (Table 3). The model shown almost flawless prediction abilities especially in Classes 7, 8, and 5, where *d* and *r* values approached unity (0.99 and 0.98 respectively). In climate modeling, particularly in dry and semi-arid areas where little changes in water availability or temperature can have significant effects on ecosystem stability, such high degrees of agreement

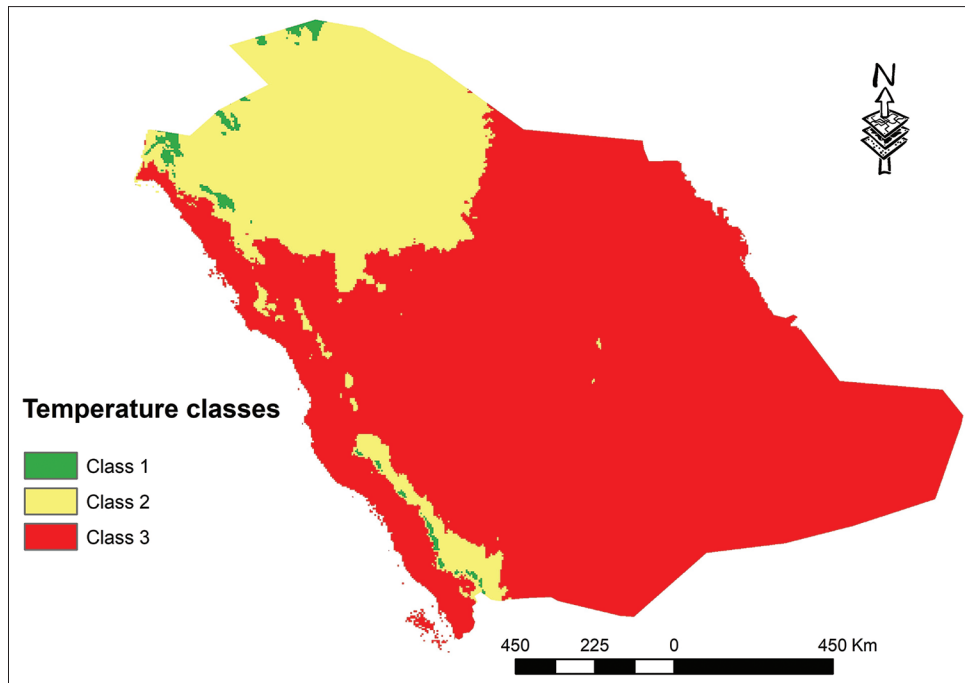


**Figure 2:** Represents the temperature classification map of the KSA

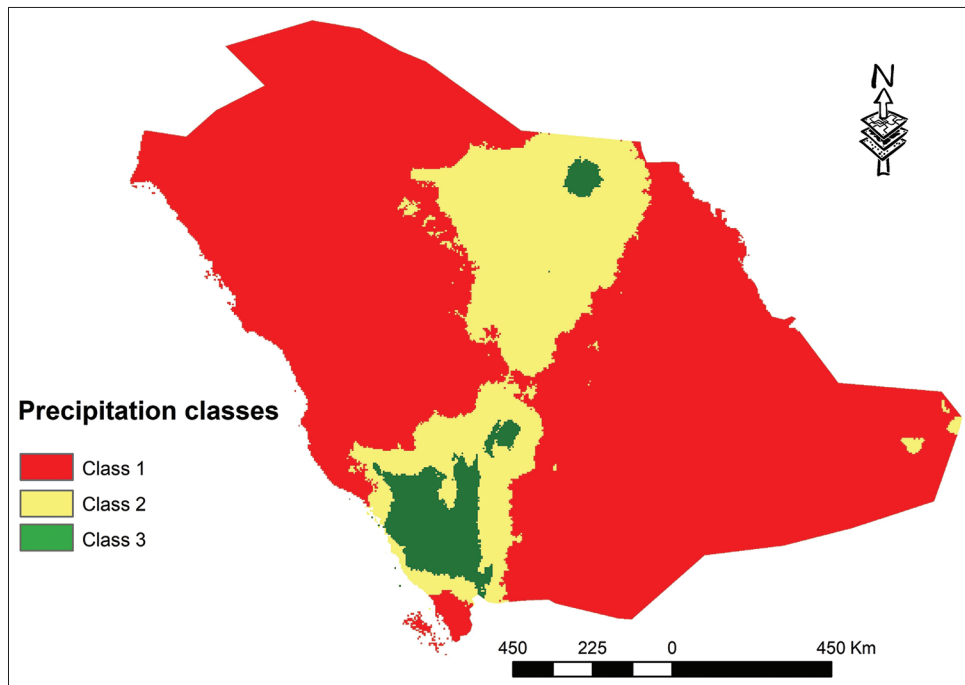


**Figure 3:** Represents the precipitation classification map of the KSA

are vital (Mahmoud *et al.*, 2023). Consistently near to zero across all classes, the Mean Relative Error (MRE) values indicate that the SARE model is essentially unbiased in its predictions that is, neither routinely overestimates nor underestimates important outputs. Increased microclimatic complexity in high-altitude areas, where localized events like fog, cloud development, and heterogeneous vegetation may introduce variability not fully captured by the model, could be responsible for the minor negative bias noted in cooler and wetter classes, including

Class 1 (MRE=-0.1). Normalized Root Mean Square Error (NRMSE) values also fell between 0.08 to 0.27, which are low and reasonable for investigations of environmental modeling. Particularly in demanding climatic situations, NRMSE values less than 0.3 usually indicate strong model performance fit for operational and strategic uses (Peel *et al.*, 2007). One interesting finding is the range in model accuracy depending on different environmental conditions. While cooler and more humid areas (Class 1 and Class 3) showed rather lower validation scores,

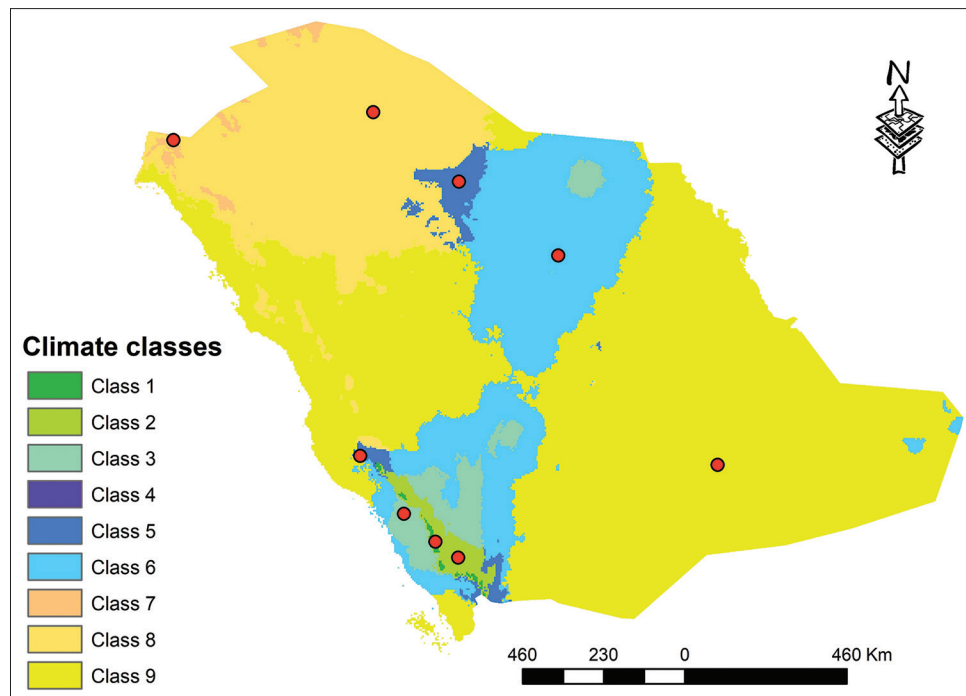


**Figure 4:** Represents the climate classification map based on long term (last 25 years) precipitation and temperature, and the red points represent the selected locations for the nine climate classes across the KSA

**Table 3:** Validation parameters of the results of SARE model against FPM model in the selected locations in the Figure 4 for the nine climate classes

Classes	D	MRE	NRMSE	R
Class 1	0.72	-0.1	0.27	0.81
Class 2	0.78	0.07	0.18	0.85
Class 3	0.74	-0.02	0.22	0.8
Class 4	0.87	-0.11	0.2	0.96
Class 5	0.91	-0.05	0.15	0.98
Class 6	0.87	-0.08	0.18	0.96
Class 7	0.99	0.01	0.08	0.99
Class 8	0.93	-0.04	0.14	0.98
Class 9	0.92	0.01	0.13	0.95

hot and hyper-arid classes, that is Class 7 and Class 8 showed the best accuracy. This distinction most likely results from the greater climatic homogeneity of desert habitats as opposed to the intricate diversity of mountainous or coastal areas. Because fewer unmodeled variables (Haq & Khan, 2022) models such as SARE can get great accuracy in hyper-arid zones whereby precipitation and temperature are regularly extreme and steady throughout time. On the other hand, in areas where orographic effects and seasonal fluctuations are more evident, more model inputs such as soil moisture dynamics or vegetation indices may be required to improve prediction accuracy even more.

The great validation performance of the SARE model has important consequences for the water and agricultural planning of Saudi Arabia. Having a consistent model that can effectively anticipate hydro-thermal conditions across many microclimates is priceless as climate change keeps aggravating evapotranspiration rates and lowering accessible water resources in arid zones. Future climate scenario analysis,

crop compatibility modeling, and irrigation scheduling under evolving environmental conditions all benefit from the SARE model’s ability to faithfully replicate the field conditions over nine different climate classes. Its validation against a strong field-based model (FPM) especially improves its legitimacy for application by water resource managers, agricultural engineers, and legislators operating in data-limited conditions.

Ultimately, the validation of the SARE model over the several climatic classes shows its resilience, adaptability, and great predictive capacity. The model performs quite well overall, matching well with observed data and surpassing usual error thresholds found in similar agroclimatic studies, despite small restrictions in colder and wetter zones. Additional environmental variables could help to improve the model for mountainous areas by means of which generalizability is enhanced even more. The SARE model stands out as a potential solution for aiding sustainable agricultural development and efficient water resource management across the Kingdom and other comparable environments internationally given the progressively pressing demand for exact climate modeling tools in arid areas.

### The Impact of Climate Classification on Evapotranspiration Variability

Significant diversity in the regulating climatic elements is revealed by the investigation of the correlation coefficients between meteorological parameters and reference evapotranspiration (ET<sub>o</sub>) computed by the SARE model over nine climate classes in Saudi Arabia. Emphasizing their fundamental importance in evapotranspiration dynamics, maximum temperature (T<sub>max</sub>)

and solar radiation (Srad) routinely show substantial positive connections across all climatic classes (Table 4). Whereas Srad exhibits equally strong correlations, reaching 0.96 in Class 7, Tmax shows correlation coefficients ranging from 0.78 in Class 1 (cold, moist) to 0.98 in Classes 5 and 8 (hotter, drier zones). These findings are in line with those of Mahmoud *et al.* (2023), who found that the main driver of evapotranspiration in arid and semi-arid climates is energy availability, mostly controlled by temperature and solar radiation.

Though its influence is rather less than that of Tmax, the minimum temperature (Tmin) also shows a clear positive association with ETo across all classes. Whereas in hotter classes like Class 5 and 8 the Tmin-ETo correlation rises to 0.98, in colder classes like Class 3 the correlation falls to 0.67. This implies that managing water loss by evapotranspiration depends more on nighttime and daytime temperatures in hotter, hyper-arid areas. On the other hand, in milder surroundings, Tmin’s importance becomes secondary, most likely because of more stable nighttime atmospheric conditions and smaller daily temperature ranges (El-Rawy *et al.*, 2023). When simulating evapotranspiration variability over several climatic zones, this pattern emphasizes the relevance of temperature extremes rather than averages.

Among the investigated meteorological factors, wind speed (WS) shows the lowest and most erratic relationships with ETo. With ranges from 0.28 in Class 4 to 0.60 in Class 1, WS correlations with ETo remain moderate to weak across all classes. Especially in cooler, more humid zones (Class 1), WS has a somewhat stronger impact on evapotranspiration than in hyper-arid zones (Class 6 and 9), in which wind plays a less role. This outcome is consistent with the theory that in very dry climates, vapor pressure deficits are already rather substantial, and more wind has a limited incremental impact on raising evapotranspiration rates (Haq & Khan, 2022). On the other hand, in more humid environments, wind can greatly increase evapotranspiration and help to move moisture.

Strongly negative connection between relative humidity (RH) and ETo across all climate classes confirms its function as a suppressor of evapotranspiration. The range of the correlation coefficients is -0.70 in Class 3 to as low as -0.96 in Class 5 and Class 8. Stronger negative associations in hotter and drier classes (Class 5, Class 8, Class 9) suggest that lower humidity levels greatly enhance the atmospheric demand for moisture, so

supporting greater evapotranspiration rates (Peel *et al.*, 2007). This is expected since dry air conditions accelerate water loss by raising the vapor pressure gradient between the land surface and the atmosphere. The very strong negative associations seen in Classes 5 and 8 imply that even little variations in RH can significantly influence ETo in hyper-arid areas, which is essential for water management and irrigation planning.

### CONCLUSION

This work highlights the significant and diverse influence of climatic elements on the reference evapotranspiration (ETo) across various climate zones in Saudi Arabia. With correlation values as high as 0.98 and 0.96, respectively, especially in hyper-arid areas like Classes 5, 7, and 8. Maximum temperature (Tmax) and sun radiation (Srad) were found by statistical analysis to be the main drivers of evapotranspiration fluctuation. Minimum temperature (Tmin) also showed strong positive effects, reaching up to 0.98 in hotter climates, thus underlining the increased importance of both daytime and nighttime temperatures in reducing water loss in extreme conditions. Conversely, wind speed (WS) showed only modest to weak connections; the highest r value (0.60) was found in cooler, more humid climates (Class 1), therefore reinforcing its secondary influence, which reduces in hyper-arid zones where vapor pressure deficits are already maximum. With correlations as low as -0.96 in the driest and hottest classes, relative humidity (RH) constantly showed a strong negative influence on ETo. In hyper-arid conditions, when dropping humidity levels greatly increase evapotranspiration rates, this inverse link becomes crucial. These results imply that any water resource management plan for drylands has to include closely watched RH and be based on it. Crucially, the variability of these influences across nine well-defined climate classes, obtained by means of a strong long-term climate classification system based on TerraClimate data, emphasizes that no single modeling technique can sufficiently reflect evapotranspiration behavior across all environments. Verified with high reliability metrics (r ranging from 0.80 to 0.99 and NRMSE values between 0.08 and 0.27), the performance of the SARE model supports the need for climate-specific model tuning. Emphasizing the difficulty presented by microclimatic complexity in mountainous and coastal areas, Classes 5, 7, and 8 showed particularly exceptional model accuracy (r = 0.98-0.99), while slightly lower performance was noted in cooler, more humid zones. This study reveals valuable insights about hyper-arid areas, which cover most of Saudi Arabia and demand great accuracy in evapotranspiration modeling because small errors could lead to significant inefficiencies in water use a critical issue where “every drop count” (Haq & Khan, 2022; Mahmoud *et al.*, 2023). Therefore, our work supports the use of specialized evapotranspiration models catered to the hydro-thermal conditions of various climate zones instead of depending on broad, homogeneous models. The complicated interaction among meteorological parameters across spatial gradients requires a more sophisticated approach to water conservation legislation, irrigation scheduling, and agricultural planning (Arafa *et al.*, 2024). Particularly in transition zones, future studies could improve models by including other environmental

**Table 4: correlation coefficient (r) of weather parameters against ETo calculated by SARE model for every climate class in KSA, to detect varying effects of weather parameters on ETo Variability for every climate class**

Parameters	R								
	Class 1	Class 2	Class 3	Class 4	Class 5	Class 6	Class 7	Class 8	Class 9
Tmax	0.78	0.85	0.79	0.94	0.98	0.98	0.96	0.98	0.97
Tmin	0.72	0.83	0.67	0.9	0.98	0.97	0.96	0.98	0.96
WS	0.6	0.54	0.36	0.28	0.5	0.32	0.49	0.49	0.37
Srad	0.84	0.84	0.9	0.94	0.95	0.93	0.96	0.94	0.79
RH	-0.77	-0.75	-0.7	-0.87	-0.96	-0.94	-0.91	-0.96	-0.93



parameters, such as soil moisture and vegetation indices. In the end, a better knowledge of the dynamic controls of ETo provides a strategic benefit for guaranteeing sustainable water resource management and food security in arid and semi-arid surroundings under the pressure of climate change.

## LIMITATIONS AND FUTURE RESEARCH DIRECTIONS

This study provides valuable insights into the impact of weather on ETo across various regions of Saudi Arabia, yet it also presents certain limitations. The study primarily utilized TerraClimate datasets and excluded high-resolution ground-based measurements, which could have detected minor changes, particularly in microclimatic zones. Omitting factors such as soil texture, crop type, and irrigation methods may render the results less valuable for agricultural decision-making. The study also concentrated on long-term climate averages, which may not accurately reflect the impact of short-term weather extremes or abrupt climate anomalies. Subsequent investigations ought to address these issues by integrating data from diverse sources, including vegetation indices derived from remote sensing, soil moisture profiles, and real-time meteorological information. Furthermore, examining the applicability of the SARE model in other arid and semi-arid regions, along with its potential adaptation to future climate change, could enhance its utility in global water resource management.

## REFERENCES

- Abdelraouf, R. E., El-Shawadfy, M. A., Bakry, A. B., Abdelaal, H. K., El-Shirbeny, M. A., Ragab, R., & Belopukhov, S. L. (2024). Estimating ETO and scheduling crop irrigation using Blaney-Criddle equation when only air-temperature data are available and solving the issue of missing meteorological data in Egypt. *BIO Web of Conferences* (Vol. 82, Article 02020). EDP Sciences. <https://doi.org/10.1051/bioconf/20248202020>
- Afify, N. M., El-Shirbeny, M. A., El-Wesemy, A. F., & Nabil, M. (2023). Analyzing satellite data time-series for agricultural expansion and its water consumption in an arid region: A case study of the Farafra Oasis in Egypt's Western Desert. *Euro-Mediterranean Journal for Environmental Integration*, 8(1), 129-142. <https://doi.org/10.1007/s41207-022-00340-4>
- Ajjur, S. B., & Al-Ghamdi, S. G. (2021). Evapotranspiration and water availability response to climate change in the Middle East and North Africa. *Climatic Change*, 166(3), 28. <https://doi.org/10.1007/s10584-021-03122-z>
- Alhathloul, S. H., Khan, A. A., & Mishra, A. K. (2024). Temporal variability of temperature, precipitation, drought, and their potential influence on horizontal visibility over Saudi Arabia. *Theoretical and Applied Climatology*, 155(12), 4621-4639. <https://doi.org/10.1007/s00704-024-04906-w>
- Allen, R. G., Pereira, L. S., Raes, D., & Smith, M. (1998). *Crop Evapotranspiration-Guidelines for Computing Crop Water Requirements-FAO Irrigation and Drainage Paper 56*. Rome, Italy: FAO.
- Al-Wabel, M. I., Sallam, A., Ahmad, M., Elanazi, K., & Usman, A. R. A. (2020). Extent of climate change in Saudi Arabia and its impacts on agriculture: A case study from Qassim Region. In S. Fahad, J. Saud, C. Wu, D. Adnan, M. A. Turan & M. Ul-Allah (Eds.), *Environment, Climate, Plant and Vegetation Growth* (pp. 557-572) Cham: Springer. [https://doi.org/10.1007/978-3-030-49732-3\\_25](https://doi.org/10.1007/978-3-030-49732-3_25)
- Arafa, Y., El-Gindy, A.-G. M., El-Shirbeny, M., Bourouah, M., Abd-ElGawad, A. M., Rashad, Y. M., Hafez, M., & Youssef, M. A. (2024). Improving the spatial deployment of the soil moisture sensors in smart irrigation systems using GIS. *Cogent Food & Agriculture*, 10(1), 2361124. <https://doi.org/10.1080/23311932.2024.2361124>
- Bindajam, A. A., Mallick, J., AlQadhi, S., Singh, C. K., & Hang, H. T. (2020). Impacts of vegetation and topography on land surface temperature variability over the semi-arid mountain cities of Saudi Arabia. *Atmosphere*, 11(7), 762. <https://doi.org/10.3390/atmos11070762>
- Derardja, B., Khadra, R., Abdelmoneim, A. A. A., El-Shirbeny, M. A., Valsamidis, T., De Pasquale, V., & Deflorio, A. M. (2024). Advancements in remote sensing for evapotranspiration estimation: A comprehensive review of temperature-based models. *Remote Sensing*, 16(11), 1927. <https://doi.org/10.3390/rs16111927>
- Eid, A. R., Fathy, M., El-Sayed, A., Hafez, M., El-Shirbeny, M. A., Reda, A. M., Mady, A. Y., Ramadan, A., Fathy, M., El-Sayed, A., Hafez, M., Ahmed, M., El-Shirbeny, M. A., & Reda, A. M. (2023). Validation of SALT-MAD model for simulating soil moisture and faba bean productivity under deficit irrigation and integrated fertilization in the semi-arid regions. *Soil & Environment*, 42(2), 111-129. <https://doi.org/10.25252/SE/2023/242926>
- Elnesr, M., & Alazba, A. (2013). Effect of climate change on spatiotemporal variability and trends of evapotranspiration, and its impact on water resources management in the Kingdom of Saudi Arabia. In B. R. Singh (Ed.), *Climate Change - Realities, Impacts Over Ice Cap, Sea Level and Risks* (pp. 273-296) USA: InTech. <https://doi.org/10.5772/54832>
- Elnesr, M., Alazba, A., & Abu-Zreig, M. (2010). Spatio-temporal variability of evapotranspiration over the Kingdom of Saudi Arabia. *Applied Engineering in Agriculture*, 26(5), 833-842. <https://doi.org/10.13031/2013.34944>
- El-Rawy, M., Batelaan, O., Al-Arifi, N., Alotaibi, A., Abdalla, F., & Gabr, M. E. (2023). Climate change impacts on water resources in arid and semi-arid regions: A case study in Saudi Arabia. *Water*, 15(3), 606. <https://doi.org/10.3390/w15030606>
- El-Shirbeny, M. A., & Abdellatif, B. (2017). Reference evapotranspiration borders maps of Egypt based on kriging spatial statistics method. *International Journal of GEOMATE*, 13(37), 1-8. <https://doi.org/10.21660/2017.37.63048>
- El-Shirbeny, M. A., & Abutaleb, K. A. (2018). Monitoring of water-level fluctuation of Lake Nasser using altimetry satellite data. *Earth Systems and Environment*, 2(4), 367-375. <https://doi.org/10.1007/s41748-018-0069-5>
- El-Shirbeny, M. A., & Biradar, C. (2024). Advances in earth observation and artificial intelligence in monitoring vegetation dynamics of dryland agroecosystems. In A. Srivastava, P. K. Aggarwal & P. D. Singh (Eds.), *Vegetation Dynamics and Crop Stress* (pp. 1-19) Cambridge, Massachusetts: Academic Press. <https://doi.org/10.1016/B978-0-323-95616-1.00001-8>
- El-Shirbeny, M. A., & Orlandini, S. (2023). Monitoring of crop water consumption changing based on remotely sensed data and techniques in North Sinai, Egypt. *Journal of Aridland Agriculture*, 9, 1-8. <https://doi.org/10.25081/jaa.2023.v9.7464>
- El-Shirbeny, M. A., & Saleh, S. M. (2021). Actual evapotranspiration evaluation based on multi-sensed data. *Journal of Aridland Agriculture*, 7, 95-102. <https://doi.org/10.25081/jaa.2021.v7.7087>
- El-Shirbeny, M. A., Abdellatif, B., Ali, A. E. M., & Saleh, N. H. (2016). Evaluation of Hargreaves based on remote sensing method to estimate potential crop evapotranspiration. *International Journal of GEOMATE*, 11(23), 2143-2149. <https://doi.org/10.21660/2016.23.1122>
- El-Shirbeny, M. A., Aboelghar, M. A., Arafat, S. M., & El-Gindy, A. M. (2014). Assessment of the mutual impact between climate and vegetation cover using NOAA-AVHRR and Landsat data in Egypt. *Arabian Journal of Geosciences*, 7(4), 1287-1296. <https://doi.org/10.1007/s12517-012-0791-3>
- El-Shirbeny, M. A., Ali, A. M., Khder, G. A., Saleh, N. H., Afify, N. M., Badr, M. A., & Bauomy, E. M. (2021a). Monitoring agricultural water in the desert environment of New Valley Governorate for sustainable agricultural development: A case study of Kharga. *Euro-Mediterranean Journal for Environmental Integration*, 6, 56. <https://doi.org/10.1007/s41207-021-00256-5>
- El-Shirbeny, M. A., Ali, A. M., Savin, I., Poddubskiy, A., & Dokukin, P. (2021b). Agricultural water monitoring for water management under pivot irrigation system using spatial techniques. *Earth Systems and Environment*, 5, 341-351. <https://doi.org/10.1007/s41748-020-00164-8>
- El-Shirbeny, M. A., Alsersy, M. A., Saleh, N. H., & Abu-Taleb, K. A. (2015). Changes in irrigation water consumption in the Nile Delta of Egypt assessed by remote sensing. *Arabian Journal of Geosciences*, 8, 10509-10519. <https://doi.org/10.1007/s12517-015-2005-2>

- El-Shirbeny, M. A., Biradar, C., Amer, K., & Paul, S. (2022). Evapotranspiration and vegetation cover classifications maps based on cloud computing at the Arab countries scale. *Earth Systems and Environment*, 6(4), 837-849. <https://doi.org/10.1007/s41748-022-00320-2>
- El-Shirbeny, M. A., Hendawy, E. A., Baioumy, E. M., Elbana, M., Gamal, R., & Abou-Hadid, A. F. (2025). Cloud computing random forest classification for major agricultural crops in the Nile Delta of Egypt. *Euro-Mediterranean Journal for Environmental Integration*. <https://doi.org/10.1007/s41207-025-00899-8>
- El-Shirbeny, M. A., Mohamed, E. S., & Negm, A. (2019). Estimation of crops water consumptions using remote sensing with case studies from Egypt. In A. Negm (Ed.), *Conventional Water Resources and Agriculture in Egypt* (pp. 451-469) Cham, Switzerland: Springer International Publishing. [https://doi.org/10.1007/978-94-007-698-2\\_20](https://doi.org/10.1007/978-94-007-698-2_20)
- Gamal, R., El-Shirbeny, M., Abou-Hadid, A., Swelam, A., El-Gindy, A. G., Arafa, Y., & Nangia, V. (2022). Identification and quantification of actual evapotranspiration using integrated satellite data for sustainable water management in dry areas. *Agronomy*, 12(9), 2143. <https://doi.org/10.3390/agronomy12092143>
- Haq, M. A., & Khan, M. Y. A. (2022). Crop water requirements with changing climate in an arid region of Saudi Arabia. *Sustainability*, 14(20), 13554. <https://doi.org/10.3390/su142013554>
- IPCC. (2021). *AR6 Climate Change 2021: The Physical Science Basis*. Intergovernmental Panel on Climate Change. <https://www.ipcc.ch/report/ar6/wg1>
- Komurcu, M., Schlosser, C. A., Alshehri, I., Alshahrani, T., Alhayaza, W., AlSaati, A., & Strzepek, K. (2020). Mid-century changes in the mean and extreme climate in the Kingdom of Saudi Arabia and implications for water harvesting and climate adaptation. *Atmosphere*, 11(10), 1068. <https://doi.org/10.3390/atmos11101068>
- Köppen, W. (1936). Das geographische System der Klimate. *Gebrüder Borntraeger*, 1, 1-44.
- Mahmoud, S. H., Gan, T. Y., & Zhu, D. Z. (2023). Impacts of climate change and climate variability on water resources and drought in an arid region and possible resiliency and adaptation measures against climate warming. *Climate Dynamics*, 61, 4079-4105. <https://doi.org/10.1007/s00382-023-06795-7>
- Monteith, J. L. (1965). Evaporation and environment. *Symposia of the Society for Experimental Biology*, 19, 205-234.
- Moriasi, D., Arnold, J., Van Liew, M., Bingner, R., Harmel, R., & Veith, T. (2007). Model evaluation guidelines for systematic quantification of accuracy in watershed simulations. *Transactions of the ASABE*, 50(3), 885-900. <https://doi.org/10.13031/2013.23153>
- Peel, M. C., Finlayson, B. L., & McMahon, T. A. (2007). Updated world map of the Köppen-Geiger climate classification. *Hydrology and Earth System Sciences*, 11(5), 1633-1644. <https://doi.org/10.5194/hess-11-1633-2007>
- Penman, H. L. (1948). Natural evaporation from open water, bare soil and grass. *Proceedings of the Royal Society A*, 193, 120-146.
- Tolba, R. A., El-Shirbeny, M. A., Abou-Shleel, S. M., & El-Mohandes, M. A. (2020). Rice acreage delineation in the Nile Delta based on thermal signature. *Earth Systems and Environment*, 4, 287-296. <https://doi.org/10.1007/s41748-019-00132-x>
- Willmott, C. J. (1982) Some Comments on the Evaluation of Model Performance. *Bulletin of the American Meteorological Society*, 63, 1309-1313. [https://doi.org/10.1175/1520-0477\(1982\)063%3C1309:SCOTEO%3E2.0.CO;2](https://doi.org/10.1175/1520-0477(1982)063%3C1309:SCOTEO%3E2.0.CO;2)
- Youssef, M. A., Peters, R. T., El-Shirbeny, M., Abd-ElGawad, A. M., Rashad, Y. M., Hafez, M., & Arafa, Y. (2024). Enhancing irrigation water management based on ETo prediction using machine learning to mitigate climate change. *Cogent Food & Agriculture*, 10(1), 2348697. <https://doi.org/10.1080/23311932.2024.2348697>